



Research Paper

Effects of backbone cyclization on the pharmacokinetics and drug efficiency of the orally active analgesic conotoxin cVc1.1



Aaron G. Poth^a, Francis C.K. Chiu^c, Sofie Stalmans^d, Brett R. Hamilton^{b,e}, Yen-Hua Huang^a, David M. Shackelford^c, Rahul Patil^c, Thao T. Le^a, Meng-Wei Kan^a, Thomas Durek^a, Evelien Wynendaele^d, Bart De Spiegeleer^d, Andrew K. Powell^c, Deon J. Venter^e, Richard J. Clark^f, Susan A. Charman^c, David J. Craik^{a,*}

^a Institute for Molecular Bioscience, Australian Research Council Centre of Excellence for Innovations in Peptide and Protein Science, The University of Queensland, Brisbane 4072, Australia

^b Center for Microscopy and Microanalysis, The University of Queensland, Brisbane 4072, Australia

^c Centre for Drug Candidate Optimisation, Monash Institute of Pharmaceutical Sciences, Monash University, Parkville 3052, Australia

^d Drug Quality and Registration (DruQuaR) Group, Ghent University, Ghent 9000, Belgium

^e Mater Health Services, Pathology Department, South Brisbane 4101, Australia

^f School of Biomedical Sciences, The University of Queensland, Brisbane 4072, Australia

ARTICLE INFO

Article history:

Received 29 December 2020

Received in revised form 25 February 2021

Accepted 27 February 2021

Available online 8 March 2021

Keywords:

Conotoxin

Cyclic peptides

Pharmacokinetics

Bioavailability

Drug efficiency index

ABSTRACT

Chronic pain is an undertreated epidemic affecting quality of life in at least 20% of the global population, and CNS-related side effects, tolerance, and addiction are common features of current medications. α -Conotoxin Vc1.1 potently elicits prolonged analgesia in preclinical chronic constriction injury and chronic visceral hypersensitivity models of neuropathic pain. A backbone-cyclized variant, cVc1.1, exhibits superior in vitro stability and is orally active, but its in vivo half-life and disposition, both critical in informing drug candidate progression, remain unexplored. Here, we investigate the pharmacological influence of the peptidic bridge differentiating linear and cyclic Vc1.1 in various pre-clinical PK/PD rodent models. While previous in vitro studies had indicated cyclization conferred increased stability for cVc1.1, in vivo the peptides exhibited similar half-lives and oral bioavailabilities. The ratios of free drug exposure metrics ($C_{max} \times f_{u,p}$ and $AUC_{0-inf} \times f_{u,p}$) following oral dosing vs. their respective in vitro IC_{50} s at the GABA_B receptor were comparable for Vc1.1 and cVc1.1, indicating similar drug efficiency indexes. MALDI imaging, radiolabel, and LC-MS biodistribution studies of cVc1.1 in rodents demonstrated that the intact cyclopeptide and several metabolites persist in the GI tract for at least 4 h, long after the plasma levels of the intact peptide had fallen below the target IC_{50} . Biodistribution analyses of IV administered ¹²⁵I-labelled cVc1.1 revealed accumulation primarily in the kidneys consistent with renal elimination, and combined with insignificant uptake in brain, suggested a low likelihood of CNS-related side effects.

1. Introduction

Disulfide-rich and macrocyclic peptides are attractive starting points in drug design due to their resistance to degradation in vitro and demonstrated high selectivity compared with small molecule drugs [1–3]. Conotoxins are a hypervariable group of disulfide-rich peptides that are the principal bioactive constituents in the venoms of predatory marine cone snails [4]. Conotoxins are integral to the snails' highly evolved defense and prey-capture strategies, and work by targeting ion channels to block signaling [5–10]. Conotoxins are classified into diverse structural subfamilies, membership of which is primarily governed by the lengths of their inter-cysteine loops and disulfide connectivities. α -Conotoxins that target nicotinic acetylcholine receptors (nAChRs) and arise from genes belonging

to the A-superfamily [11], exhibit a type I cysteine framework (CC-C-C) with two disulfide bonds between Cys^I-Cys^{III} and Cys^{II} and Cys^{IV}. Their respective inter-cysteine loops vary in size and composition [12] and are key determinants of α -conotoxin selectivity toward a range of neuronal- and muscle-type nAChRs, as well as the GABA_B receptor, which enables them to regulate high-voltage calcium channel currents in sensory neurons [13].

Several conotoxins target receptors involved in nociception and accordingly have analgesic activity [14]. This property, along with the promise of in vivo stability due to their disulfide-braced structures, has led to efforts to develop pain therapeutics, including ω -conotoxin MVIIA (ziconotide)—a drug that received FDA approval in 2004 for the treatment of enduring pain unable to be addressed with opioids [15,16], and CVID—which reached clinical trials for the treatment of neuropathic pain [17].

* Corresponding author at: Institute for Molecular Bioscience, The University of Queensland, Brisbane, Queensland 4072, Australia.

E-mail address: d.craik@imb.uq.edu.au (D.J. Craik).

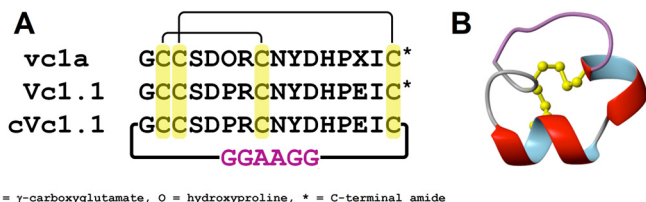


Figure 1. Structure of cVc1.1 and related peptides. (A) Sequence alignment and posttranslational modifications of α -conotoxins vcl1a, Vc1.1 and cVc1.1. (B) Three-dimensional model of cVc1.1. Backbone cyclization of cVc1.1 is achieved through the incorporation of a peptide linker (purple) joining the N- and C-termini of Vc1.1. All peptides have the same disulfide connectivity, as indicated at the top of the figure.

Conotoxin Vc1.1 (Figure 1) is a modified synthetic form of the 16 amino acid α -conotoxin Vc1a from the venom of *Conus victoriae* [18,19], which demonstrates striking activity in animal models of neuropathic pain [20,21], eliciting long-lasting analgesia measurable for at least 24 h following a single subcutaneous dose. Vc1.1 underwent development by Metabolic Pharmaceuticals as a treatment for neuropathic pain and progressed through double-blinded phase 1 clinical trials, demonstrating no drug-related adverse effects when administered subcutaneously at up to 0.8 mg kg⁻¹ per day in healthy male volunteers, with a dose-proportional pharmacokinetic profile [22]. However, a phase 2A clinical trial in patients with sciatic neuropathic pain was abandoned after contemporaneous *in vitro* investigations determined that Vc1.1 was significantly less potent at the human form of its presumed target, the $\alpha 9\alpha 10$ nAChR than had earlier been observed for the rat isoform [23], halting further commercial development [22,24].

In 2008, Callaghan et al. demonstrated that Vc1.1 is a potent inhibitor of GABA_B-receptor (GABA_BR)-linked N-type (Ca_v2.2) calcium channel currents, offering an alternative hypothesis for the analgesic mechanism [13]. Subsequently, we reported the design, synthesis, and oral activity of a backbone-cyclized variant, cVc1.1, which incorporates a 6-amino acid residue linker joining the N- and C-termini of Vc1.1 [21]. Cyclized Vc1.1 had higher potency in inhibition of high voltage-activated Ca²⁺ channel currents compared to linear Vc1.1 (IC₅₀s of 0.3 nM and 1.7 nM, respectively), but a lower potency for inhibition of $\alpha 9\alpha 10$ nAChRs (IC₅₀s of 64 nM and 766 nM, respectively). Conotoxin cVc1.1 was able to elicit sustained analgesia in rat chronic constriction injury (CCI) assays following oral administration and was more potent than gabapentin [21], the current gold standard treatment for management of neuropathic pain. Furthermore, in a mouse chronic visceral hypersensitivity (CVH) model, cVc1.1 was more effective in reducing pseudo-related pain responses than Vc1.1 [25]. Despite intense interest in the development of novel α -conotoxins for use in the clinic, these peptides have only been well-characterized in *in vitro* studies, and there remains limited preclinical pharmacokinetic and disposition data for these drug candidates in the literature.

Peptides face some challenges in their development as therapeutics due to their susceptibility to enzymatic degradation, typically poor permeability and large molecular size [26]. So far, efforts to improve oral absorption of conotoxins have centered around conjugation of lipophilic substituents on α -conotoxin MII, eliciting marked improvements in permeability across Caco-2 cell monolayers [27] and were reported to exhibit oral bioavailability in radio-biodistribution assays [28]. However, the radioactivity measurements reported [28] for MII do not necessarily correspond uniquely to the presence of the intact peptide, leaving unanswered questions about molecular longevity, disposition, and biological fate of intact conotoxins *in vivo*. As a part of the preclinical evaluation of novel therapeutics, it is important to gain insight into their biodistribution, for instance in the case of chemotherapeutic cancer drugs where effective management of the condition relies upon appropriate maintenance within the bounds of the therapeutic window. Furthermore, biodistribution studies are conducted with

the intent to derisk drug development by monitoring for unusual patterns or toxic accumulation (e.g., nephrotoxicity) [29]. Typically, this has been achieved through the use of whole body autoradiography or organ homogenate analysis; however, the former method lacks the ability to distinguish between intact therapeutics, and the latter cannot convey fine-grained detail on biodistribution [30].

While initial work on backbone-cyclized conotoxins [21,31–33] demonstrated their superior stability to degradation *in vitro* serum stability and intestinal fluid assays, as for many investigations of putative peptide therapeutics [34], it remains to be established whether these results translate into longer half-life *in vivo*. Separately, where conventional drug lead/candidate optimization processes rely on sequential and typically siloed efforts to improve potency, physicochemical and other ADME properties, there is a risk of overlooking compounds with an overall favorable drug profile but which might not be carried to the next round of optimization due to a perceived failing in one category. This can be captured by use of the drug efficiency index (DEI) [35–37], which corresponds inversely with required clinical dose, and which thereby can be used as a basis for comparison of candidate analogs for a given target, and also for comparison across drug classes.

Here, we evaluate the effects of backbone cyclization on the *in vivo* pharmacokinetics and biodistribution of Vc1.1 in rodents. Furthermore, we sought to determine whether cyclization conferred a holistic advantage to this peptide drug as judged by the drug efficiency (D_{eff}) and DEI parameters, and to put these values in context with the calculated metrics for several marketed therapeutics. LC-MS biodistribution and MALDI imaging studies of orally dosed mice demonstrated that cVc1.1 and several metabolites persisted in the GI tract for at least as long as the duration of action previously observed in CCI assays and long after the plasma levels of the parent molecule had fallen below the limit of detection. Biodistribution of ¹²⁵I-labelled cVc1.1 after IV administration was also investigated. Overall, this study elucidates the *in vivo* pharmacokinetic and biodistribution data on an intact therapeutic conotoxin, and supports the hypothesis that the long-lived analgesic effects of cVc1.1 might at least in part be mediated by the persistence of active metabolites generated *in vivo*, or from the action of trace levels of the intact molecule upon systemic GABA_BRs localized exclusive of the brain.

2. Materials and methods

2.1. Peptide synthesis

Peptides were purchased from American Peptide Company, Inc. (Sunnyvale, CA, USA) and validated to be >95% purity (Figure S1) using LC-MS on a Shimadzu Prominence system eluted over 30 min with a linear acetonitrile:water (0.05% formic acid) gradient (1–60%) delivered at a flow rate of 0.3 mL min⁻¹ and on a Applied Biosystems 4700 MALDI-TOF spectrometer.

2.2. PK studies for Vc1.1 and cVc1.1 in rats

The intravenous (IV) and oral pharmacokinetic profiles of Vc1.1 and cVc1.1 were assessed in fasted male Sprague Dawley rats. All procedures were approved by the Monash Institute of Pharmaceutical Sciences Animal Ethics Committee and conducted in accordance with the Australian Code for the Care and Use of Animals for Scientific Purposes.

2.3. Formulation preparation and analysis

IV Formulations: Each compound was dissolved in saline forming clear colorless solutions with a pH of 3.1 for cVc1.1 and 3.0 for Vc1.1. The formulations were filtered through 0.22 μ m syringe filters prior to dosing, and the average measured concentration of compound in aliquots ($n = 2$) of the filtered solutions was 3.48 mg mL⁻¹ for cVc1.1 and 2.49 mg mL⁻¹ for Vc1.1. Negligible adsorption of either peptide to the filter membranes was observed. Oral Formulations: Each compound was dissolved in Milli-Q H₂O

forming a clear colorless solution with a pH of 3.0 for cVc1.1 and 2.7 for Vc1.1. The average measured concentration of compound in aliquots ($n = 3$) of the solutions was 5.30 mg mL^{-1} for cVc1.1 and 4.42 mg mL^{-1} for Vc1.1.

2.4. Pharmacokinetic study details

The pharmacokinetics of cVc1.1 and Vc1.1 were studied in overnight-fasted male Sprague Dawley rats weighing 281–295 g. Rats had access to water ad libitum throughout the pre- and postdose sampling period, and access to food was reinstated 4 h postdose. cVc1.1 and Vc1.1 were each administered intravenously as a 10 min constant rate infusion via an indwelling jugular vein cannula (1 mL per rat, $n = 3$ rats per compound) and orally by gavage (10 mL/kg per rat, $n = 3$ rats per compound), and samples of arterial blood and urine were collected up to 7 h postdose. At each sample time, a single 220 μL sample of arterial blood was collected from each rat into a borosilicate vial (at 4°C) containing heparin, Complete® (a protease inhibitor cocktail) and potassium fluoride to minimize potential for *ex vivo* degradation of cVc1.1 or Vc1.1. Blood samples were centrifuged to obtain plasma, and 100 μL of plasma from each blood sample was combined for the three rats in each group to obtain 300 μL pooled samples for LC-MS analysis. Where less than 100 μL of plasma could be separated from a blood sample, the maximum available volume was added to the pooled sample to maximize the volume of plasma available for analysis. Across all pooled samples, the lowest volume added to the pool was 70 μL , and the impact of this reduced volume on the overall concentration in the pooled sample was minimal and deemed acceptable for the purposes of this exploratory pharmacokinetic study. Urine from each rat was collected into chilled vials as pooled samples over the periods of 0–7 h and 7–24 h. Plasma and urine samples were then frozen and stored at -80°C (for a maximum of 10 days) until analysis by LC-MS. Negligible degradation of either peptide was observed in stability studies when spiked into blood, plasma, or urine matrices and maintained at RT for 2 h, 4°C for 48 h, or following a single freeze-thaw cycle (-80°C to RT).

2.5. Bioanalytical methods

All samples for quantitative analysis were spiked with internal standard. Prior to LC-MS, analytes were extracted from PK plasma samples using solid-phase extraction. Waters Oasis HLB 30 mg cartridges were activated with 1 mL methanol and then equilibrated with 1 mL Milli-Q water. To measure total analyte in PK samples, 300 μL of plasma was loaded onto each cartridge, followed with 1 mL Milli-Q water. The analyte was eluted with 1 mL of 50% acetonitrile in water followed by 300 μL of 2% ammonium hydroxide in acetonitrile into a fresh micro centrifuge tube. The combined eluent was evaporated to dryness using a Turbovap concentrator at 45°C under continuous nitrogen flow. The dried samples were reconstituted with 50 μL of 10% methanol in water and transferred to polypropylene sample vial for analysis. Recovery for all analytes was $>75\%$ and matrix effect between 80 and 120% over the range of quantitation.

For plasma protein-binding assays, samples were subjected to protein precipitation using a 3:1 (v:v) methanol, and the supernatant collected following sample centrifugation at $13,000 \times g$ for 10 mins. Urine samples were treated and diluted (20 or 200-fold) with 10% methanol:water and analyzed directly. All other formulations were diluted in 10% methanol:water to within the calibration range.

LC-MS analyses were performed using a Waters Acquity UPLC system interfaced with a Waters Xevo TQD operating in positive electrospray ionization multiple reaction monitoring mode. In each run, 10 μL injections were made to a Supelco Ascentis Express RP C18 column ($50 \times 2.1 \text{ mm}$, $2.7 \mu\text{m}$ particle size), and samples were eluted over 6 min with a linear acetonitrile:water (0.05% formic acid) gradient delivered at a flow rate of 0.6 mL min^{-1} . Instrument settings including MRM transitions are provided in Table S1.

2.6. Calculation of pharmacokinetic parameters

Plasma concentration vs. time data were analyzed using noncompartmental methods (PKSolver Version 2.0). Standard calculations for each pharmacokinetic parameter are listed below.

$$\text{Plasma CL} = \frac{\text{Dose}_{IV}}{\text{AUC}_{IV}} \quad (1)$$

$$\text{Plasma } V_{ss} = \frac{\text{AUMC}_{IV}}{\text{AUC}_{IV}} \cdot \text{Plasma CL} \quad (2)$$

$$\text{BA} = \frac{\text{AUC}_{oral} \times \text{Dose}_{IV}}{\text{AUC}_{IV} \times \text{Dose}_{oral}} \times 100\% \quad (3)$$

Oral bioavailability (BA) was also estimated on the basis of the urinary recovery data as:

$$\text{BA} = \frac{f_{e,unchanged}^{oral}}{f_{e,unchanged}^{IV}} \times 100\% \quad (4)$$

where $f_{e,unchanged}$ is the fraction of the IV or oral dose recovered in urine as unchanged compound over the 24 h postdose sampling period. A standard deviation (SD) for the apparent oral bioavailability based on urine data was calculated using the propagation of errors approach [38].

2.7. Protein-binding assay details

Plasma protein binding was assessed by ultracentrifugation using a modification of a method reported previously by Nakai et al. [39]. Briefly, rat plasma (male Sprague Dawley) was spiked with cVc1.1 or Vc1.1 (in 10% v/v methanol in Milli-Q water) to a nominal compound concentration of $1 \mu\text{M}$, and the final methanol concentration was 0.1% (v/v). After vortex mixing, aliquots ($n = 6$) of spiked plasma were transferred into ultracentrifuge tubes and subjected to ultracentrifugation at 37°C (Beckman Rotor type 42.2 Ti; $223,000 \times g$) for 4.2 h to separate proteins. Following ultracentrifugation, an aliquot of protein-free supernatant was taken from each of the ultracentrifuge tubes to obtain measures of the unbound concentration ($C_{unbound}$). Additional ultracentrifuge tubes ($n = 4$; noncentrifuged) containing spiked plasma were maintained at 37°C for 0.5 h and 4.2 h, and the concentrations at the two timepoints were compared to assess compound stability, as well as to obtain a measure of the total compound concentration in plasma at 4.2 h (C_{total}). All samples were stored frozen at -80°C until analysis by LC-MS. A summary of the bioanalytical method and assay validation details is included in Supplementary Information.

The unbound fraction (f_u) of cVc1.1 and Vc1.1 in rat plasma was calculated using the average values for C_{total} and $C_{unbound}$ as per the following equation:

$$f_u = \frac{C_{unbound}}{C_{total}} \quad (5)$$

Based on measured compound concentrations in PK plasma samples ($C_{plasma-total}$) and fraction unbound value (f_u), unbound plasma concentrations ($C_{plasma-unbound}$) were calculated as:

$$C_{plasma-unbound} = C_{plasma-total} \times f_u \quad (6)$$

2.8. Drug efficiency metrics

Drug efficiency metrics were calculated using the following equations from Braggio et al. [35] and Valko et al. [36]:

$$D_{eff} = 100 \times \frac{[\text{Drug}]_{biophase} \left(\frac{\text{mg}}{\text{mL}} \right)}{[\text{Dose}] \left(\frac{\text{mg}}{\text{g}} \right)} \quad (7)$$

$$D_{\text{eff max}} = 100 \times \frac{[\text{Drug}]_{\text{free plasma}} \left(\frac{\text{mg}}{\text{mL}} \right)}{[\text{Dose}] \left(\frac{\text{mg}}{\text{g}} \right)} \quad (8)$$

$$\text{DEI} = \log D_{\text{eff}} + \text{pIC}_{50} \quad (9)$$

2.9. MALDI imaging of cVc1.1 in orally dosed mice

Juvenile C57BL/6 males (3 weeks) were administered cVc1.1 dissolved in PBS via oral gavage at a rate of 20 mg kg⁻¹ and returned to their accommodation with ad libitum access to food and water. At time points of 0, 10, 60 and 240 min ($n = 3$ per time point), individuals were sacrificed with CO₂ and immediately snap-frozen in dry ice and hexane baths (-95 °C) for 15 min and then stored at -80 °C. Individuals were positioned atop a custom cryosectioning chuck and frozen in place in a bath of water prior to sectioning at 30 μm using a Leica CM3050S. Intact whole-mount axial longitudinal sections were transferred individually to Bruker Indium Tin Oxide (ITO)-treated glass slides (BrukerDaltonik) and allowed to air dry for 12 h under reduced pressure. Dry sections were defatted via extensive washing with DCM. Defatted dry sections were coated with CHCA (α-cyano-4-hydroxycinnamic acid) prepared at 7 mg mL⁻¹ in 50% ACN/0.1% TFA using a Bruker ImagePrep system. Optical images of the prepared slides were collected using an Epson Expression 10,000 XL scanner. MALDI-MSI was conducted on a BrukerUltraflex III MALDI-TOF/TOF instrument controlled by Flex Control 3.3 and Flex Imaging 4.0. Spectra were acquired over the mass range m/z 750–4000 with a 200 μm raster over the section areas, and data were analyzed using FlexImaging software.

2.10. MS analysis of individual rat tissues after oral dosing

Following acclimatization, juvenile male Wistars (6–8 weeks, $n = 15$) were administered cVc1.1 dissolved in water via oral gavage at a dose of 10 mg kg⁻¹. At predetermined time points of 0, 10, 30, 60 and 120 min following administration, cohorts ($n = 3$) were euthanized with CO₂ and immediately dissected to yield sample tissues and organs: lung, heart, liver, kidney, brain, spleen, small intestine, large intestine, bladder, which were kept on ice prior to storage at -80 °C until further analysis. Collected tissues were homogenized in PBS (10 mL g⁻¹ tissue) using an IKA Ultratarrax, and the solutions were immediately clarified using a refrigerated benchtop centrifuge. Bioanalytical preparation was conducted using Oasis HLB SPE cartridges as detailed in the above PK section. Samples were subsequently analyzed in an IDA experiment conducted via LC-MS/MS on a SCIEX TripleTOF 5600 instrument as detailed previously.

2.11. Brain penetration of cVc1.1

2.11.1. Preparation of ¹²⁵I radiolabeled cVc1.1

The cyclic toxin peptide, cVc1.1, was radiolabeled using the chloramine T method iodinating the Y (Tyr) amino acid, described below:

To 50 μL of 1 μmol mL⁻¹ cVc1.1 solution in 5% ACN (v/v) + 0.1% formic acid was added 20 μL of a 3.75 μmol mL⁻¹ I NaI solution in aqueous 0.1% FA in a LoBind Eppendorf tube. To this was added a volume of Na¹²⁵I solution equivalent to 1 mCi of Na¹²⁵I, followed by 30 μL of 0.5 mg mL⁻¹ CAT solution in 130 mM phosphate buffer (pH 7.4). After 40 s of iodination reaction time, the reaction was quenched via the addition of 30 μL of a 1 mg mL⁻¹ sodium metabisulfite solution in phosphate buffer 130 mM (pH 7.4).

After radiolabeling, the ¹²⁵I cVc1.1 was fractionated using a linear acetonitrile gradient on a Vydac C18 Everest column (4.6 × 250 mm, 5 μm particle size) using a radio-HPLC system consisting of a LaChrom Elite L-2130 pump with degasser, a LaChrom Elite L-2300 column oven, a LaChrom Elite L-2400 UV detector (all Hitachi, Tokyo, Japan), a Rheodyne 7725i manual injector with 100 μL sample loop (Rheodyne, Rohnert Park, CA, USA), and a Berthold LB500 HERM radioactivity detector (Berthold Technologies, Bad Wildbad, Germany) equipped with EZChrom Elite Version software for data acquisition (Scientific Software, Pleasanton, CA,

USA). The selected radiolabeled peptide fractions were evaporated using a N₂ flow in order to obtain a ¹²⁵I-peptide stock solution.

2.11.2. Brain preparation

Caesarean Derived-1 (CD-1) mouse brain was collected in ice-cold Krebs buffer and prepared as previously detailed for use in binding studies [40,41]. Briefly, mouse plasma was obtained from Harlan Laboratories, while mouse brain homogenate was prepared as described previously by Vergote et al. [42]. In brief, brain was collected from male ICR-CD-1 mice, cleaned and washed in ice-cold Krebs-Henseleit buffer pH 7.4 and about 1.5 g was transferred to 50 mL rotor-stator disperser tubes. Then, 36 mL of ice-cold Krebs-Henseleit buffer were added and the organs were homogenized with an IKA Ultra-Turrax (Staufen, Germany) for one minute. After sedimentation for 30 min at 5 °C to remove the larger particles, 25 mL of the middle layer were taken as final homogenate, with aliquots stored at -35 °C until further use. Prior to use, the protein content of each homogenate was determined using the Pierce-modified Lowry Protein Assay method (Thermo Scientific, Erembodegem, Belgium) to generate a stock solution with a protein concentration of 0.6 mg mL⁻¹ by dilution with Krebs-Henseleit buffer.

2.11.3. Multiple time regression influx study

Multiple time regression (MTR) analyses were conducted to evaluate the ability of the peptide to cross the blood brain barrier, with methods as described elsewhere in detail [40,41]. Briefly, ICR-CD-1 mice were anesthetized intraperitoneally using a 40% urethane solution (3 g kg⁻¹). The jugular vein and carotid artery were isolated, and 200 μL of the radiolabeled peptide solution, diluted to 30,000 cpm μL⁻¹ using lactated Ringer's solution containing 1% BSA (LRBSA⁻¹), was injected into the jugular vein. At specified time points after injection (1, 3, 5, 10, 12.5 and 15 min, with start and end in replicates), blood was obtained from the carotid artery followed by decapitation of the mouse. The isolated brain was weighed and radioactivity measured in a gamma counter (Wallac Wizard automatic gamma counter, Perkin Elmer, Shelton, CT, USA), as well as from 50 μL serum, which was obtained by centrifuging the collected blood at 10,000 × g for 15 min at 21 °C. To evaluate the tissue distribution of the peptides during the BBB experiments, eight tissues, that is, spleen, kidneys, lungs, heart, liver, intestines, bladder, and stomach, were collected immediately after decapitation of the mice at the last time point of 15 min. After weighing the tissues, the radioactivity was measured in a gamma counter. The linear modeling of the MTR analysis is based on the Gjedde-Patlak equation [43,44].

$$\frac{A_m(t)}{C_p(t)} = K_{in} \frac{\int_0^t C_p(t) \cdot dt}{C_p(t)} + V_i \quad (10)$$

where $A_m(t)$ is the amount of radioactivity in the brain at time t , $C_p(t)$ the amount of radioactivity in serum at time t , K_{in} the brain influx rate constant and V_i the initial brain distribution volume. Due to clearance of intravenously injected drugs before reaching the brain during MTR experiments, exposure time is used in modeling brain influx to account for the decreasing concentrations. The exposure time (exp time) represents the theoretical steady-state serum level of radiolabeled peptide at the serum concentration $C_p(t)$ and is defined as the integral of the serum radioactivity over time divided by the radioactivity at time t :

$$\text{exp time} = \frac{\int_0^t C_p(t) \cdot dt}{C_p(t)} \quad (11)$$

The integral of radioactivity over time is represented by the area under the curve (AUC). Finally, the brain serum⁻¹ ratios (μL g⁻¹) were plotted vs. the exposure time and the slope of the linear portion of this relationship measures the unidirectional influx rate (K_{in}) from blood to brain, whereas the intercept represents the initial brain volume of distribution (V_i). For the evaluation of the tissue distribution of the radiolabeled peptide

15 min after IV-injection, the percentage of the injected dose for each isolated tissue is calculated as per Eq. (12).

$$\% \text{injected dose} = \frac{A_{\text{tissue}}/W_{\text{tissue}}}{A_{\text{injected}}/W_{\text{animal}}} \times 100 \quad (12)$$

where A_{tissue} and A_{injected} are the measured activity of the isolated tissue and the activity of 200 μL of MTR stock solution, respectively, while w_{tissue} is the weight of the considered tissue and w_{animal} is the mass of the injected mouse.

2.11.4. Capillary depletion

Capillary depletion experiments were conducted to assess the extent to which the peptide could cross into the parenchyma after permeating the BBB epithelium, using the method of Triguero et al. as modified by Gutierrez et al. [41,45,46]. Briefly, ICR-CD-1 mice were first IP anesthetized using a 40% urethane solution (3 g kg^{-1}). The jugular vein was isolated and into this, 200 μL of the iodinated peptide solution, diluted to $10,000 \text{ cpm } \mu\text{L}^{-1}$ using LR/BSA, was injected. Blood samples were collected from the abdominal aorta 10 min post injection and the brain was perfused manually with 20 mL of lactated Ringer's buffer after clamping the aorta and severing the jugular veins. Following this, the brain was collected and weighed, and its radioactivity was measured using a gamma counter. Then the brain was homogenized with 0.7 mL of ice-cold capillary buffer (10 mM HEPES, 141 mM NaCl, 4 mM KCl, 2.8 mM CaCl_2 , 1 mM MgSO_4 , 1 mM NaH_2PO_4 , and 10 mM D-glucose adjusted to pH 7.4) in a pyrex glass tube and mixed with 1.7 mL of 26% ice-cold dextran solution in capillary buffer. The resulting solution was weighed and centrifuged in a swinging bucket rotor at $4500 \times g$ for 30 min at 4°C , after which the radioactivity was measured using a gamma counter. Pellet (capillaries) and supernatant (parenchyma and fat tissue) were also collected and weighed before gamma counter measurements were taken. Finally, the radioactivity of 50 μL of serum was also measured in a gamma counter after centrifuging the collected blood sample ($10,000 \times g$, 21°C , 15 min). Compartmental distribution was calculated as per Eq. (13).

$$\text{Fraction} = \frac{CD_{\text{tissue}}}{\frac{A_{\text{capillaries}}}{A_{\text{serum}}} + \frac{A_{\text{parenchyma}}}{A_{\text{serum}}}} \times 100 \quad (13)$$

where CD_{tissue} represents the ratio of activity in the capillaries or parenchyma vs. activity in serum for the fraction of radiolabeled peptide in the capillaries or parenchyma, respectively.

2.11.5. Brain-blood transport

This method was performed to quantify the amount of peptide pumped out of the brain by efflux transport as previously described [47]. ICR-CD-1 mice were anesthetized intraperitoneally using a 40% urethane solution (3 g kg^{-1}). The skin of the skull was removed and a hole was made into the lateral ventricle using a 22 G needle marked with tape at 2 mm at the following coordinates: 1 mm lateral and

0.34 mm posterior to the bregma. The anesthetized mice received an intracerebroventricular (ICV) injection of 1 μL of the diluted iodinated peptide solution using LR/BSA ($25,000 \text{ cpm } \mu\text{L}^{-1}$) by pumping the peptide solution at a speed of $360 \mu\text{L h}^{-1}$ for 10 s using a syringe pump (KDS100, KR analytical, Cheshire, UK). At specified time-points after ICV injection (1, 3, 5, 10, 12.5 and 15 min), blood was collected from the abdominal aorta and subsequently the mouse was decapitated. Then, the whole brain was collected, weighed, and measured in a gamma counter, as well as from 50 μL of serum, which was obtained by centrifuging the collected blood at $10,000 \times g$ during 15 min at 21°C . The efflux half-life was calculated from the linear regression of the natural logarithm of the residual radioactivity in brain vs. time as per Eq. (14).

$$t_{1/2} = \frac{\ln(2)}{k_{\text{out}}} \quad (14)$$

where k_{out} is defined as the efflux rate constant calculated as the negative value of the slope of the linear regression, applying first-order kinetics.

3. Results

3.1. Linear Vc1.1 and backbone-cyclized cVc1.1 exhibit similar terminal half-lives and low oral bioavailability in rats

Previous comparison of Vc1.1 and cVc1.1 in vitro serum stability assays demonstrated a higher resistance to degradation for the latter peptide. To evaluate the influence of peptide backbone cyclization upon in vivo pharmacological properties, the peptides were compared in a rat pharmacokinetic model. Synthetic Vc1.1 and cVc1.1 peptides of purity $>95\%$ (Figure S1) were used in all experiments. Being an exploratory pharmacokinetic study, samples were collected only across a limited number of time points, and due to limitations in sensitivity for the analytes, it was necessary to pool the triplicate biological replicates prior to analysis. Following IV administration to rats, plasma concentrations of both Vc1.1 and cVc1.1 were quantifiable using MS-based multiple reaction monitoring (Tables S1–S3) for up to 5 h, but neither concentration-time profile exhibited a clearly defined terminal phase and half-lives could only be estimated (see Figure 2). Following oral administration, maximal plasma concentrations were observed at the earliest sampling timepoint, and total exposure of Vc1.1 (based on total concentrations in plasma) was shown to be being higher than that for cVc1.1 (Figure 2A and B). For Vc1.1, fluctuations in the latter portion of the IV profile precluded an accurate estimation of the terminal half-life, but comparison of the PO time-course measurements suggests broadly similar rates of elimination for the peptides. While both Vc1.1 and cVc1.1 exhibited low volumes of distribution (Table 1), plasma clearance of Vc1.1 was lower than that of cVc1.1. Urinary recovery data indicated that renal elimination accounted for approximately 50% of the overall in vivo clearance of both compounds (Table S4). As both peptides were bound to plasma proteins to a similar extent (Table S5), the same trend in plasma exposure was evident in the calculated unbound plasma

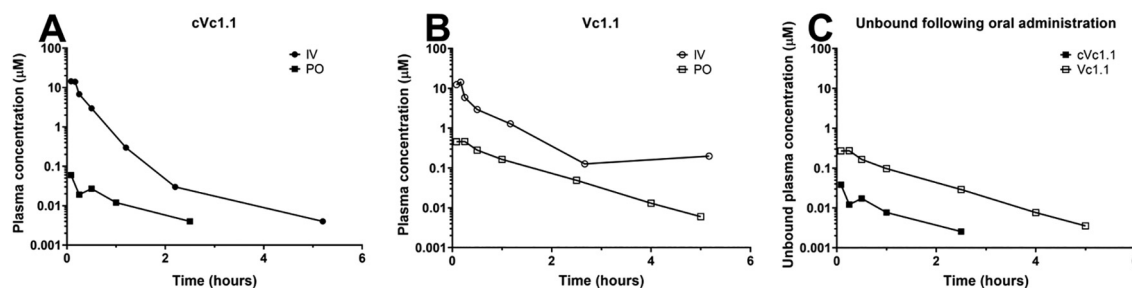


Figure 2. Comparison of cVc1.1 and Vc1.1 pharmacokinetics in rats. Plasma concentrations of (A) cVc1.1 and (B) Vc1.1 based on analysis of pooled samples ($n = 3$ per time point) from male Sprague Dawley rats after IV and oral administration. (C) Comparison of calculated unbound plasma concentrations of cVc1.1 and Vc1.1 in male Sprague Dawley rats following oral administration using the fraction unbound data in Table S5.

Table 1

Plasma pharmacokinetic parameters for cVc1.1 and Vc1.1 in male Sprague Dawley rats after IV and oral administration^a

Parameter	cVc1.1		Vc1.1	
	Intravenous	Oral	Intravenous	Oral
Average measured dose (mg kg ⁻¹)	12.4	53.0	8.6	45.0
Apparent T _{1/2} (mins)	39*	49	72†	50
Plasma clearance (mL min ⁻¹ kg ⁻¹)	20	–	13	–
Plasma V _{ss} (L kg ⁻¹)	0.3	–	0.4	–
Plasma C _{max} (μM)	–	0.060	–	0.46
T _{max} (min)	–	5	–	15
Plasma AUC _{0-∞} (μM.h)	4.75	0.040	6.32	0.49
% of dose in urine‡	45.1 ± 2.6	0.14 ± 0.04	53.0 ± 13.3	0.7 ± 0.6
Apparent bioavailability (%) based on plasma AUC	–	0.2	–	1.5
Apparent bioavailability (%) based on urinary recovery	–	0.31 ± 0.09	–	1.2 ± 1.1

* Because the terminal phase was not clearly defined, this value is an approximation only, and may underestimate the actual half-life of cVc1.1.

† Value is an approximation only based on the last 4 points of the profile. As the half-life after oral administration cannot be shorter than that after IV dosing, it is likely that this value is an overestimation of the actual IV half-life of Vc1.1.

‡ Recovery in urine as unchanged peptide over 24 h.

Table 2

Drug potency and efficiency metrics for cVc1.1 and Vc1.1

Metric	cVc1.1	Vc1.1	Cyclosporin A	Calcitonin
D _{eff} (%)*	0.16	1.09	1.17	0.81
D _{effmax} (%)†	160	177	N/A	N/A
DEI‡	8.71	8.80	8.22	8.94
Log D _{eff}	-0.80	0.03	0.07	-0.09
pIC ₅₀	9.52§	8.77§	8.15	9.03
T _{1/2}	0.82¶ (3.3#)	0.83¶ (3.3#)	19**	0.25**

* D_{eff}, Drug efficiency.

† D_{effmax}, Maximal drug efficiency.

‡ DEI, Drug efficiency index.

§ At GABA_B receptors.

|| Terminal phase half-life (hours).

¶ In rats (hours).

Approximation in humans (hours) via allometric scaling [49].

** In humans (hour).

exposure profiles (Figure 2C). Based on plasma AUC and urinary recovery data, the apparent oral bioavailability for cVc1.1 was 0.2–0.3% and for Vc1.1 was 1.2%–1.5% (Table 1). However, the observed difference in bioavailability (based on urinary excretion data) between cVc1.1 and Vc1.1

failed to reach statistical significance ($p > 0.05$, unpaired t -test), indicating that the two peptides exhibited similar bioavailabilities.

3.2. Drug efficiency metrics of Vc1.1 and cVc1.1 are not dissimilar from marketed peptide and small molecule drugs

To assess the developability potential of peptide drug candidates, we sought to calculate and compare the DEI of cVc1.1 and Vc1.1 with examples of “within-class” peptide drugs. The DEI is a measure of the proportion of occupied vs. unoccupied receptors per unit of dose and serves as a key pivot point between potency and drug efficiency in early drug development about which efforts to reduce general toxicity are focused [35,37,48]. As summarized in Table 2 and Eqs. (7)–(9), the drug efficiency is derived from only dose, maximal free drug exposure at the site of action and target potency values. Here, unbound concentrations in plasma provide a surrogate measure of the free drug exposure at a tissue-resident site of action, assuming that distribution of cVc1.1 and Vc1.1 into tissues occurs via passive diffusion and is not impacted by active uptake or efflux processes.

The calculated drug efficiency metrics of Vc1.1 and cVc1.1 were found to exhibit outline similarity with those for marketed peptide drugs cyclosporin A and calcitonin, spanning D_{eff} values between 0.16 and 1.17%. The increased potency of cVc1.1 over Vc1.1 at its pharmacological target [21], the GABA_B receptor, is largely offset by its reduced oral bioavailability as inferred through a combination of PK and urinary recovery data, resulting in essentially equivalent DEIs.

Both Vc1.1 and cVc1.1 exhibited a pIC₅₀/DEI ratio close to unity, and compare favorably among values calculated for 115 marketed small molecule drug compounds [36]; the peptides' relative positions suggesting the likelihood for favorable in vivo PK/PD profiles, and a higher likelihood to be efficacious at lower dose. Furthermore, allometric scaling of half-life in rats suggests a half-life in the order of several hours in humans (Table 2).

3.3. ¹²⁵I biodistribution and brain penetration of cVc1.1

To help assess the safety profile of cVc1.1, we conducted exploratory radiobiodistribution assays in mice. As shown in Figure 3, following IV administration, BSA exhibited distribution primarily in the serum and liver, while dermorphin as a control model peptide [50] was mainly distributed to the liver and small intestines. Dermorphin is an opioid peptide and binds opioid receptors present in the small intestine, consistent with its high representation in this tissue. For cVc1.1, the tissue distribution 15 min after IV injection showed that it was mainly present in the kidneys and to a lesser extent in serum. The radioactivity in serum (corrected for injected dose) is plotted vs. time in Figure S2. Tissue influx and peptide elimination are indicated by the decrease in the ratio of the serum activity over the IV injected activity within 15 min. The approximate 2/3 drop in cVc1.1 in mice over 15 min is not dissimilar to the greater than 50% drop

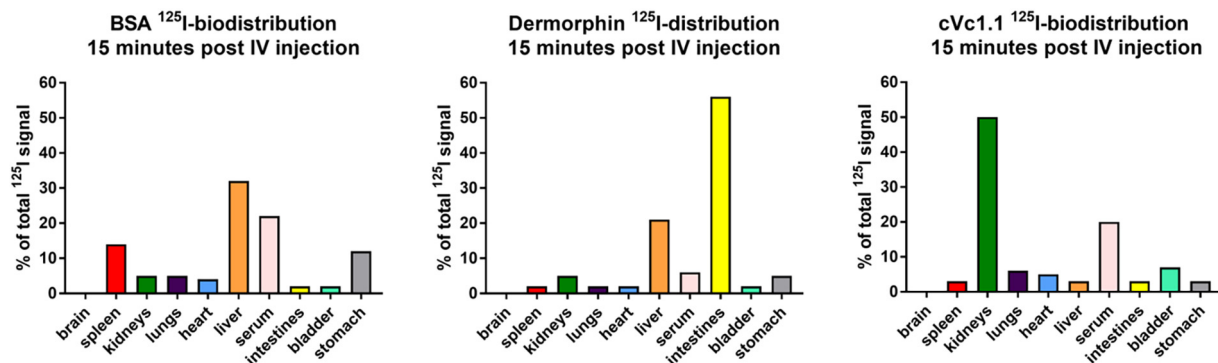


Figure 3. Biodistribution of ¹²⁵I-labelled BSA, dermorphin and cVc1.1 in mice 15 min post IV administration. Percentage ID (injected dose) is the ratio of the activity of the respective tissue, corrected for its mass, and the injected activity, corrected for the mouse weight ($n = 2$).

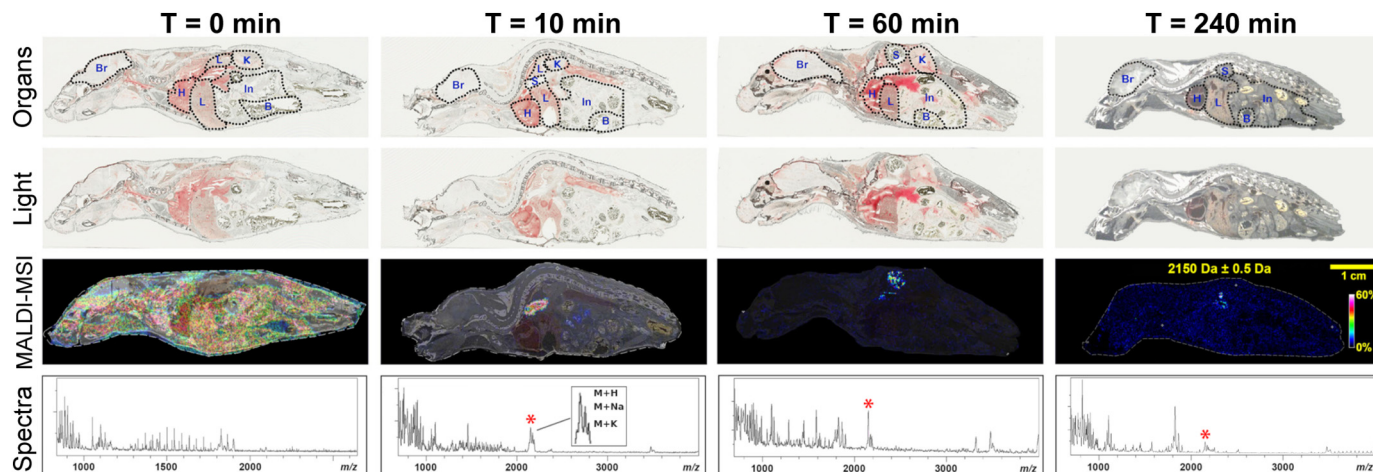


Figure 4. Time-course of spatial biodistribution heatmaps for cVc1.1 via MALDI-imaging of orally dosed C57BL/6 mice. Top row—labelled light microscopic images with major organs; second row—unaltered scanned images of longitudinal sections; third row—MALDI-MSI signal intensity heatmaps for cVc1.1 (m/z 2150 Da) overlaid with the light image; bottom row—Average spectra indicating the presence of intact peptide ($M + H$) and related $M + Na$ and $M + K$ adduct ions (clusters indicated by red asterisks) in dosed rodents. Br = brain; S = stomach; L = liver; K = kidney; B = bladder; H = heart; In = intestine.

in cVc1.1 observed in rats following IV administration: from 31.0 ng/mL at 5 min to 14.6 ng/mL at 25 min (see Tables S6 and S7 for Vc1.1).

3.4. Biodistribution of cVc1.1 in orally dosed rodents is principally detectable within the stomach and small intestine

To check for inappropriate or unexpected drug distribution, a combination of organ homogenate analyses and MALDI-MSI visualization approaches was utilized to examine the biodistribution of cVc1.1 in multiple rodent species. Given the oral activity of cVc1.1, biodistribution studies were conducted following oral administration of cVc1.1 in juvenile Wistar rats, using a combination of MALDI-MSI and organ homogenate analyses. Tissue homogenates were produced from cohorts sacrificed over a time-course and analyzed via LC-MS to quantify cVc1.1. As summarized in Figure S3, the intact peptide was detected primarily in the stomach and some in small intestine, with negligible signal in the other sampled tissues.

Mass spectrometry imaging (MSI) was used to investigate the localization of cVc1.1 in axial longitudinal sections of 3-week-old juvenile C57BL/6 mice having received the peptide via oral gavage. In control experiments, cVc1.1 was spiked onto blank mouse sections and resultant MALDI-TOF analysis of these samples registered signals for the peptide with a delta mass of approximately -10 Da. This mass difference is presumably influenced by the topography and thickness of the section, which shifts the analyte closer to the detector. When analyzed as spotted directly onto a polished steel MALDI target with CHCA matrix, signals for cVc1.1 were observed with a monoisotopic $M + H$ signal at m/z 2159.5, whereas the average signal for cVc1.1 generated directly from the tissue section was detected at m/z 2150 Da (Figure S4).

Representative MALDI-MSI heatmaps shown in Figure 4 illustrate the localization of intact cVc1.1 as well as signals that correspond with its sodium and potassium adducts over a time course following oral administration and demonstrate that it is present in the stomach and intestinal regions for at least 4 h, with no evidence of localization in other tissues.

Despite the low oral bioavailability of cVc1.1, it is clear from the ^{125}I -cVc1.1 radiobiodistribution study of IV-dosed rodents that significant proportions of the systemically available peptide and/or its metabolites might be present in the kidney and bladder (Figure 3), and so their nondetection may simply be a result of inherently low signal. This is in accord with the PK bioavailability data that show only a very small proportion of oral dose reaches the systemic circulation. For MALDI imaging analyses, the lack of signals outside of the gastrointestinal tract was unsurprising

given the relatively low sensitivity quantitative capability of this technique on tissue compared with unobstructed MALDI targets.

3.5. cVc1.1 exhibits negligible brain penetration in MTR influx studies

To assess the brain-penetrating properties of cVc1.1, it was subjected to a panel of blood-brain barrier transport experiments. During the MTR experiments, cVc1.1 only showed a limited influx into the mouse brain. Using the Gjedde-Patlak [43,51] linear approach, a brain influx rate constant (K_{in}) value of $0.06 \mu\text{L g}^{-1} \text{min}^{-1}$ was calculated for cVc1.1. This K_{in} is lower than the influx rate constant of the negative control BSA. Together with the small initial brain distribution volume ($V_i = 9.76 \mu\text{L g}^{-1}$), being lower than the V_i of BSA ($V_i = 12.15 \mu\text{L g}^{-1}$), cVc1.1 showed no influx into the brain. The results for BSA ($K_{in} = 0.0960 \mu\text{L g}^{-1} \text{min}^{-1}$; very low, negligible brain influx) [51] and demorphin ($K_{in} = 0.3544 \mu\text{L g}^{-1} \text{min}^{-1}$; low brain influx) correspond to previously reported results, indicating the validity of our experiments. Table S8 summarizes the MTR influx results using a linear regression model for cVc1.1 and both controls. Figure S5 illustrates the regression curves for BSA, demorphin and cVc1.1 calculated using the Gjedde-Patlak linear model. The simple linear model was sufficient given that capillary depletion results confirmed poor influxes into the brain: only a small amount of radioactivity was found in the brain tissue (i.e., $A_{\text{tissue}}/A_{\text{serum}}$ ratios < 4). For comparison, an $A_{\text{tissue}}/A_{\text{serum}}$ ratio of more than 10 was obtained during the capillary depletion study of apidaecin Apil37, which shows a high influx into the brain [40]. Of the limited amount of peptide that crossed the BBB, about 80% ($81.22\% \pm 1.04$) effectively reached the brain parenchyma, while about 20% ($18.78\% \pm 1.04$) remained in the capillaries. Figure S6 shows the distribution of cVc1.1 in brain tissue and the fractions associated with brain capillaries and parenchyma with respect to the brain homogenate (i.e., the sum of brain capillaries and parenchyma). To determine whether the BBB has directional permeability, the efflux of cVc1.1 out of the brain was evaluated, and the natural logarithm of the measured residual radioactivity in the brain is plotted vs. the sampling time points in Figure S7. The efflux transfer constant K_{out} was found to be -0.0227min^{-1} [$-0.0745, 0.0291$; 65% confidence interval] demonstrating that cVc1.1 did not show significant efflux, consistent with a lack of influx. The serum activity only shows experimental variability as a function of time, with no evidence of a significant increasing trend. In summary, these results demonstrate that for cVc1.1, there was no discernible influx into or efflux out of the brain. A summary of biological replicates is provided in Table S9.

4. Discussion

In a previous comparison of cVc1.1 and Vc1.1 in an array of in vitro plasma, gastric and intestinal stability assays, the levels of the linear peptide were seen to decline steeply by the first measurement point, possibly due to reshuffling of the disulfide bonds in the assay conditions [21], before leveling out to a slower decline. The in vivo pharmacokinetic comparison in the current study found both peptides exhibited similar rates of elimination, with terminal half-lives of ~50 min based on the orally dosed animals. This suggests that peptidic degradation processes which might be expected to be reduced by the cyclic backbone may not contribute substantially toward the overall elimination of either peptide in vivo. Aligned with this, renal elimination of intact peptide is a significant in vivo clearance pathway for both cVc1.1 and Vc1.1, with ~50% of the IV dose being recovered intact in urine.

The oral bioavailabilities estimated on the basis of both plasma exposure and relative urinary excretion after IV and oral administration were low (0.2–0.3% and 1.2–1.5% for cVc1.1 and Vc1.1, respectively). These values are significantly lower than what might be expected given the results for the homologous α -conotoxin MII and a lipidated derivative N-LaaMII [27], for which more than 6% had crossed the GI tract of rats within 30 min of administration, as observed in radiobiodistributive assays. However, these values do not specifically represent the intact peptide and would include any metabolites harboring the radiolabel, and hence might be significantly artificially elevated.

The pharmacokinetic and biophysical parameters determined for cVc1.1 and Vc1.1 indicate they share a similar degree of plasma protein binding and a small volume of distribution of $<1 \text{ L kg}^{-1}$. Hence, only a minor proportion of the administered dose distributes outside of the circulatory system. As noted elsewhere [52], it is important to recognize that the small volume of distribution does not preclude unbound peptide from accessing tissue-resident sites of action.

The DEI value of a drug represents the balance between the free unbound concentrations (C_{max}) achieved at its target, factoring in its potency at the target receptor (or the receptor occupancy per unit of dose). With plasma protein binding being essentially equal between cVc1.1 and Vc1.1, the lower bioavailability of cVc1.1 compared with Vc1.1 is counterbalanced by its higher potency at the target biophase. Studies assessing hundreds of oral drugs have found that fewer than 30% have a drug efficiency of less than 1%, with the bulk appearing in the range of 1–5%, [37,48] and on this basis, of the two examined peptides, the balance between potency and drug efficiency is closer to the majority of marketed drugs for Vc1.1. The drug efficiency metrics of cVc1.1 and Vc1.1 place them well within the bounds of developability, and already close to a sweet spot established in studies evaluating hundreds of marketed oral drugs [35,36].

There is a disconnect between the PK/PD relationship such that the neuroalgesic effect seems to persist for at least 4 h, or approximately 5 biological half-lives, which corresponds with the gold-standard washout period. Thus, further work addressing the pharmacology of the peptides' interactions with GABA_B receptor and $\alpha 9\alpha 10$ nAChRs is needed. Although GABA_B is expressed in all neurons, the site of activity is likely the dorsal root ganglion, which has no protective sheath and is highly vascularized [53,54]. While the precognitive levels of GABA_B receptor occupancy also remain to be critically assessed [55], on the basis of investigations in other neuromodulatory receptors, the minimally effective dose might correspond to a receptor occupancy of up to 90%. On the basis of the drug efficiency (D_{eff}) and DEI values determined here for cVc1.1 and Vc1.1, 90% receptor occupancy should be achievable for either peptide at an oral dose of ~1 mg kg⁻¹, and this is in accord with the results of investigations by Clark et al. [21] describing statistically significant levels of oral activity of cVc1.1 in rat CCI assays utilizing dose rates spanning 0.3 to 3.0 mg kg⁻¹.

Many studies aimed at improving the absorption properties of peptides have sought to draw inspiration from and comparison with cyclosporin A, an oral calcineurin inhibitor with an impressive 28% oral bioavailability used as an immunosuppressive drug to prevent organ rejection. However, no studies appear to have specifically investigated the drug efficiency properties of peptide drugs in relation to cyclosporin A. In renal transplant

patients, the fraction of cyclosporin A unbound in plasma ranges from 0.04 to 0.12 [56], and it is known to bind extensively to red blood cells and plasma proteins [57]. In a study assessing cyclosporin A pharmacokinetics in renal transplant patients receiving an oral dose at a rate of 15 mg kg⁻¹, the average C_{max} was 1465 $\mu\text{g L}^{-1}$, and thus the calculated drug efficiency (D_{eff}) of cyclosporin A is 1.17%, which is similar to that for Vc1.1 (1.09%) despite the large difference in F%. This is because being such a bulky molecule and incorporating multiple N-methylations, the very properties of cyclosporin A that make it bioavailable, such as its hydrophobicity, also give it undesirable distribution, metabolism, and excretion properties. Taking potency into account, both Vc1.1 and cVc1.1 have similar DEI values (8.80 and 8.71, respectively) to cyclosporin A (8.22) and salmon calcitonin (8.94), indicating that they are likely to be effective oral drugs with lower efficacious doses than is required for cyclosporin A.

MALDI-MSI, autoradiography, and LC-MS analyses were used to assess the disposition of cVc1.1 in orally dosed rodents. In orally dosed mice, signals for the intact peptide and associated sodium and potassium ions were localized in the stomach and intestinal regions only and were detectable for at least 4 h post administration. In mice receiving ¹²⁵I-labeled cVc1.1 intravenously in radiobiodistributive studies, the primary tissues in which radiation could be measured were the kidneys and serum, with none detected in the brain. LC-MS analyses of dissected organ homogenates from orally dosed rats similarly revealed no evidence of cVc1.1 in the brain, with strong signals in the stomach and less-intense signals in the intestine, in agreement with the MALDI-MSI results. Differences between the LC-MS and MALDI-MSI *ex vivo* organ homogenate and cryosection analyses of intact cVc1.1 and the radiobiodistributive results for ¹²⁵I-labeled cVc1.1 may well be due to the measurement of metabolites alongside the intact molecule in the latter. The most striking difference is in the high kidney-centric signals for ¹²⁵I-labeled cVc1.1, where no signal was detected for intact peptide in LC-MS or MALDI-MSI studies; however this might be significantly influenced by the different administration routes utilized. The incorporation of iodine would increase the lipophilicity of the peptide and thus influence its biodistribution. However, as the iodinated peptide does not enter the brain despite this increased lipophilicity, BBB influx of the unlabeled peptide would not be expected.

During the MTR experiments, cVc1.1 exhibited only very limited influx into the mouse brain. Given the insignificant signal intensities observed, influx was calculated using the Gjedde-Patlak linear approach, wherein cVc1.1 returned a K_{in} -value of 0.06 $\mu\text{L g}^{-1} \text{ min}^{-1}$, lower than that of the influx rate recorded for the negative control BSA. The initial distribution volume for cVc1.1 was also smaller than that for BSA ($V_i = 12.15 \mu\text{L g}^{-1}$) and results from the capillary depletion study also confirmed poor influx into the brain. Efflux of cVc1.1 out of the brain was also investigated and found to be minimal and nonexistent. The tissue distributions of the control compounds BSA and dermorphin corresponded well with previously performed experiments [58]. Investigation of the tissue distribution of radiolabeled cVc1.1 revealed that the highest fraction was found in the kidneys, followed by serum. The latter can be explained by their high serum stability as observed previously [21].

Essentially nil exposure of ¹²⁵I-cVc1.1 was found in the brain of intravenously dosed mice, and there was also insignificant influx in parenchyma during MTR analyses. As our studies have demonstrated that blood-brain barrier penetration is not a requirement of achieving measurable analgesia with cVc1.1, its insignificant brain exposure represents an advantage in that it is unlikely to elicit CNS-based side effects, which plague current neuro-pathic pain medicines.

5. Conclusions

The in vivo pharmacokinetics, tissue distribution, and brain penetrance of cVc1.1 and Vc1.1 were investigated. Despite the previously identified multiple hour duration of analgesia following oral administration of cVc1.1 and the long duration of effects following IV administration of Vc1.1, the elimination half-lives were of the order of 50 min in rats. An important future focus will be to determine the full analgesic time-course back

to baseline (predose pain threshold) and to identify the half-life and penetration of metabolites in target tissues and possibly block or displace with radio labeled peptides. Although these peptides have low oral bioavailabilities, they have drug efficiencies and DEI values that parameterize receptor engagement per unit dose, and which put them within the range of currently approved oral peptide drugs. These peptides are single-digit nanomolar inhibitors of the GABA_B receptor, and the use of drug efficiency metrics, such as DEI, D_{Eff}, and D_{EffMax} which properly account for the unbound drug fraction and potency on target, provide a useful measure of their developability. Even in the absence of detailed knowledge of the pharmacological target and PK/PD relationship for cVc1.1 and Vc1.1, their biological half-lives and their DEIs, which parameterize the balance between probability of target interaction, target affinity and ADME properties, are in keeping with marketed orally administered peptide drugs, and thus suggest they possess good prospects for development.

Data statement

All research data are available on reasonable request.

Ethics statement

All animal studies were conducted using established procedures in accordance with the Australian Code of Practice for the Care and Use of Animals for Scientific Purposes, and the study protocols were reviewed and approved by the University of Queensland Animal Ethics Committee or Monash Institute of Pharmaceutical Sciences Animal Ethics Committee in compliance with ARRIVE guidelines.

Funding Source

There is no funding source for this article.

CRedit author statement

Author contributions were as follows: Aaron Poth: Conceptualization, Data curation, Formal analysis, Investigation, Methodology, Validation, Writing - original draft. Francis Chiu: Conceptualization, Methodology, Data curation, Writing - original draft. Sofie Stalmans: Conceptualization, Methodology, Data curation, Writing - original draft. Brett Hamilton: Conceptualization, Methodology, Data curation, Writing - original draft. Yen-Hua Huang: Conceptualization, Methodology, Data curation, Writing - original draft. David Shackelford: Conceptualization, Methodology, Data curation, Writing - original draft. Rahul Patil: Conceptualization, Methodology, Data curation, Writing - original draft. Thao Le: Conceptualization, Methodology, Data curation, Writing - original draft. Meng-Wei Kan: Data curation, Formal analysis, Investigation, Project administration, Writing - review & editing. Thomas Durek: Conceptualization, Methodology, Data curation, Writing - original draft. Evelien Wyendaele: Conceptualization, Methodology, Data curation, Writing - original draft. Bart De Spiegeleer: Conceptualization, Methodology, Data curation, Writing - original draft. Andrew Powell: Conceptualization, Methodology, Data curation, Writing - original draft. Deon Venter: Conceptualization, Methodology, Data curation, Writing - original draft. Richard Clark: Conceptualization, Methodology, Data curation, Writing - original draft. Susan Charman: Conceptualization, Methodology, Data curation, Writing - original draft. David Craik: Conceptualization, Methodology, Data curation, Writing - original draft, Conceptualization, Data curation, Formal analysis, Funding acquisition, Investigation, Methodology, Project administration, Resources, Software, Supervision, Validation, Visualization, Roles/Writing - original draft, Writing - review & editing.

Conflict of interest

The authors declare that there are no conflicts of interest.

Acknowledgments

We acknowledge the assistance of UQBR staff for assistance with animal studies, and Alun Jones for access to the Molecular and Cellular Proteomics facility at the Institute for Molecular Bioscience, UQ. The work was supported by a Development grant from the National Health and Medical Research Council (APP1076136) and used the facilities of the Australian Research Council Centre of Excellence for Innovations in Peptide and Protein Science (CE200100012). DJC is an Australian Research Council Laureate Fellow (FL150100146). The Centre for Drug Candidate Optimisation (CDCO) is partially supported by the Monash University Technology Research Platform network and Therapeutic Innovation Australia (TIA) through the Australian Government National Collaborative Research Infrastructure Strategy (NCRIS) program.

Appendix A. Supplementary data

Supplementary data to this article can be found online at <https://doi.org/10.1016/j.medidd.2021.100087>.

References

- [1] de Veer SJ, Kan M-W, Craik DJ. Cyclotides: from structure to function. *Chem Rev.* 2019; 119:12375–421.
- [2] Wang CK, Craik DJ. Designing macrocyclic disulfide-rich peptides for biotechnological applications. *Nat Chem Biol.* 2018;14:417–27.
- [3] Góngora-Benítez M, Tulla-Puche J, Albericio F. Multifaceted roles of disulfide bonds. *Pept Therap Chem Rev.* 2014;114:901–26.
- [4] Dutertre S, Jin AH, Vetter I, Hamilton B, Sunagar K, Laverne V, et al. Evolution of separate predation- and defence-evoked venoms in carnivorous cone snails. *Nat Commun.* 2014;5:3521.
- [5] Myers RA, Cruz LJ, Rivier JE, Olivera BM. Conus peptides as chemical probes for receptors and ion channels. *Chem Rev.* 1993;93:1923–36.
- [6] McIntosh JM, Santos AD, Olivera BM. Conus peptides targeted to specific nicotinic acetylcholine receptor subtypes. *An Rev Biochem.* 1999;68:59–88.
- [7] Terlau H, Olivera BM. Conus venoms: a rich source of novel ion channel-targeted peptides. *Physiol Rev.* 2004;84:41–68.
- [8] Akondi KB, Muttenthaler M, Dutertre S, Kaas Q, Craik DJ, Lewis RJ, et al. Discovery, synthesis, and structure–activity relationships of conotoxins. *Chem Rev.* 2014;114: 5815–47.
- [9] Zoli M, Pistillo F, Gotti C. Diversity of native nicotinic receptor subtypes in mammalian brain. *Neuropharmacol.* 2015;96:302–11.
- [10] Jin A-H, Muttenthaler M, Dutertre S, Himaya SWA, Kaas Q, Craik DJ, et al. Conotoxins: chemistry and biology. *Chem Rev.* 2019;119:11510–49.
- [11] Robinson SD, Norton RS. Conotoxin gene superfamilies. *Mar Drugs.* 2014;12:6058–101.
- [12] Azam L, McIntosh JM. Alpha-conotoxins as pharmacological probes of nicotinic acetylcholine receptors. *Acta Pharmacol Sin.* 2009;30:771–83.
- [13] Callaghan B, Haythornthwaite A, Berecki G, Clark RJ, Craik DJ, Adams DJ. Analgesic α -conotoxins Vc1.1 and Rg1A inhibit N-type calcium channels in rat sensory neurons via GABA_A receptor activation. *J Neurosci.* 2008;28:10943–51.
- [14] Adams DJ, Callaghan B, Berecki G. Analgesic conotoxins: block and G protein-coupled receptor modulation of N-type (Ca_v 2.2) calcium channels. *Br J Pharmacol.* 2012;166: 486–500.
- [15] Olivera BM, Cruz LJ, de Santos V, LeCheminant GW, Griffin D, Zeikus R, et al. Neuronal calcium channel antagonists. Discrimination between calcium channel subtypes using ω -conotoxin from *Conus magus* venom. *Biochemistry.* 1987;26:2086–90.
- [16] Atanassoff PG, Hartmannsgruber MW, Thrasher J, Wermeling D, Longton W, Gaeta R, et al. Ziconotide, a new N-type calcium channel blocker, administered intrathecally for acute postoperative pain. *Reg Anesth Pain Med.* 2000;25:274–8.
- [17] Kolosov A, Goodchild CS, Cooke I. CNSB004 (Leconotide) causes antihyperalgesia without side effects when given intravenously: a comparison with ziconotide in a rat model of diabetic neuropathic pain. *Pain Med.* 2010;11:262–73.
- [18] Sandall DW, Satkunanathan N, Keays DA, Polidano MA, Liping X, Pham V, et al. A novel α -conotoxin identified by gene sequencing is active in suppressing the vascular response to selective stimulation of sensory nerves in vivo. *Biochemistry.* 2003;42:6904–11.
- [19] Jakubowski JA, Keays DA, Kelley WP, Sandall DW, Bingham JP, Livett BG, et al. Determining sequences and post-translational modifications of novel conotoxins in *Conus victoriae* using cDNA sequencing and mass spectrometry. *J Mass Spectrom.* 2004;39: 548–57.
- [20] Satkunanathan N, Livett B, Gayler K, Sandall D, Down J, Khalil Z. Alpha-conotoxin Vc1.1 alleviates neuropathic pain and accelerates functional recovery of injured neurons. *Brain Res.* 2005;1059:149–58.
- [21] Clark RJ, Jensen J, Nevin ST, Callaghan BP, Adams DJ, Craik DJ. The engineering of an orally active conotoxin for the treatment of neuropathic pain. *Angew Chem Int Ed Engl.* 2010;49:6545–8.
- [22] Pharmaceuticals M. Metabolic's pain drug ACV1 enters second phase 2 human clinical trial. *ASX Announcement;* 2007.
- [23] Azam L, McIntosh JM. Molecular basis for the differential sensitivity of rat and human α 9 α 10 nAChRs to alpha-conotoxin Rg1A. *J Neurochem.* 2012;122:1137–44.

- [24] Pharmaceuticals M. Metabolic discontinues clinical trial program for pain drug. ASX Announcement; 2007.
- [25] Castro J, Grundy L, Deiteren A, Harrington AM, O'Donnell T, Maddern J, et al. Cyclic analogues of α -conotoxin Vc1.1 inhibit colonic nociceptors and provide analgesia in a mouse model of chronic abdominal pain. *Br J Pharmacol*. 2018;175:2384–98.
- [26] Craik DJ, Fairlie DP, Liras S, Price D. The future of peptide-based drugs. *Chem Biol Drug Des*. 2013;81:136–47.
- [27] Blanchfield JT, Gallagher OP, Cros C, Lewis RJ, Alewood PF, Toth I. Oral absorption and in vivo biodistribution of alpha-conotoxin MII and a lipidic analogue. *Biochem Biophys Res Commun*. 2007;361:97–102.
- [28] Blanchfield JT, Dutton JL, Hogg RC, Gallagher OP, Craik DJ, Jones A, et al. Synthesis, structure elucidation, in vitro biological activity, toxicity, and Caco-2 cell permeability of lipophilic analogues of alpha-conotoxin MII. *J Med Chem*. 2003;46:1266–72.
- [29] Nilsson A, Forngren B, Bjurstrom S, Goodwin RJ, Basmaci E, Gustafsson I, et al. In situ mass spectrometry imaging and ex vivo characterization of renal crystalline deposits induced in multiple preclinical drug toxicology studies. *PLoS One*. 2012;7:e47353.
- [30] Castellino S, Groseclose MR, Wagner D. MALDI imaging mass spectrometry: bridging biology and chemistry in drug development. *Bioanalysis*. 2011;3:2427–41.
- [31] Armishaw CJ, Jensen AA, Balle LD, Scott KC, Sorensen L, Stromgaard K. Improving the stability of alpha-conotoxin AulB through N-to-C cyclization: the effect of linker length on stability and activity at nicotinic acetylcholine receptors. *Antioxid Redox Signal*. 2011;14:65–76.
- [32] Lovelace ES, Gunasekera S, Alvarmo C, Clark RJ, Nevin ST, Grishin AA, et al. Stabilization of alpha-conotoxin AulB: influences of disulfide connectivity and backbone cyclization. *Antioxid Redox Signal*. 2011;14:87–95.
- [33] Halai R, Callaghan B, Daly NL, Clark RJ, Adams DJ, Craik DJ. Effects of cyclization on stability, structure, and activity of alpha-conotoxin RgIA at the alpha9alpha10 nicotinic acetylcholine receptor and GABA(B) receptor. *J Med Chem*. 2011;54:6984–92.
- [34] Cavaco M, Andreu D, Castanho M. The challenge of peptide proteolytic stability studies: scarce data, difficult readability, and the need for harmonization. *Angew Chem Int Ed*. 2021;60:1686–8.
- [35] Braggio S, Montanari D, Rossi T, Ratti E. Drug efficiency: a new concept to guide lead optimization programs towards the selection of better clinical candidates. *Expert Opin Drug Discov*. 2010;5:609–18.
- [36] Valko K, Chiarparin E, Nunhuck S, Montanari D. In vitro measurement of drug efficiency index to aid early lead optimization. *J Pharm Sci*. 2012;101:4155–69.
- [37] Montanari D, Chiarparin E, Gleeson MP, Braggio S, Longhi R, Valko K, et al. Application of drug efficiency index in drug discovery: a strategy towards low therapeutic dose. *Expert Opin Drug Discov*. 2011;6:913–20.
- [38] Shackelford DM, Jansen KM. Quantifying uncertainty in the ratio of two measured variables: a recap and example. *J Pharm Sci*. 2016;105:3462–3.
- [39] Nakai D, Kumamoto K, Sakikawa C, Kosaka T, Tokui T. Evaluation of the protein binding ratio of drugs by a micro-scale ultracentrifugation method. *J Pharm Sci*. 2004;93:847–54.
- [40] Stalmans S, Wynendaele E, Bracke N, Knappe D, Hoffmann R, Peremans K, et al. Blood-brain barrier transport of short proline-rich antimicrobial peptides. *Protein Pept Lett*. 2014;21:399–406.
- [41] Stalmans S, Bracke N, Wynendaele E, Gevaert B, Peremans K, Burvenich C, et al. Cell-penetrating peptides selectively cross the blood-brain barrier in vivo. *PLoS One*. 2015;10:e0139652.
- [42] Vergote V, Van Dorpe S, Peremans K, Burvenich C, De Spiegeleer B. In vitro metabolic stability of obestatin: kinetics and identification of cleavage products. *Peptides*. 2008;29:1740–8.
- [43] Gjedde A. High- and low-affinity transport of D-glucose from blood to brain. *J Neurochem*. 1981;36:1463–71.
- [44] Patlak CS, Blasberg RG, Fenstermacher JD. Graphical evaluation of blood-to-brain transfer constants from multiple-time uptake data. *J Cereb Blood Flow Metab*. 1983;3:1–7.
- [45] Triguero D, Buciak J, Pardridge WM. Capillary depletion method for quantification of blood-brain barrier transport of circulating peptides and plasma proteins. *J Neurochem*. 1990;54:1882–8.
- [46] Gutierrez EG, Banks WA, Kastin AJ. Murine tumor necrosis factor alpha is transported from blood to brain in the mouse. *J Neuroimmunol*. 1993;47:169–76.
- [47] Banks WA, Kastin AJ. Quantifying carrier-mediated transport of peptides from the brain to the blood. *Methods Enzymol*. 1989;168:652–60.
- [48] Valko K, Teague S, Pidgeon C. In vitro membrane binding and protein binding (IAM MB/PB technology) to estimate in vivo distribution: applications in early drug discovery. *ADMET & DMPK*. 2017;5:14–38.
- [49] Caldwell GW, Masucci JA, Yan Z, Hageman W. Allometric scaling of pharmacokinetic parameters in drug discovery: can human CL, Vss and t1/2 be predicted from in-vivo rat data? *Eur J Drug Metab Pharmacokinet*. 2004;29:133–43.
- [50] Van Dorpe S, Adriaens A, Polis I, Peremans K, Van Bocxlaer J, De Spiegeleer B. Analytical characterization and comparison of the blood-brain barrier permeability of eight opioid peptides. *Peptides*. 2010;31:1390–9.
- [51] Stalmans S, Gevaert B, Wynendaele E, Nielandt J, De Tre G, Peremans K, et al. Classification of peptides according to their blood-brain barrier influx. *Protein Pept Lett*. 2015;22:768–75.
- [52] Smith DA, Beaumont K, Maurer TS, Di L. Volume of distribution in drug design. *J Med Chem*. 2015;58:5691–8.
- [53] Jimenez-Andrade JM, Herrera MB, Ghilardi JR, Vardanyan M, Melemedjian OK, Mantyh PW. Vascularization of the dorsal root ganglia and peripheral nerve of the mouse: implications for chemical-induced peripheral sensory neuropathies. *Mol Pain*. 2008;4:10.
- [54] Colombo G. GABA_B receptor. *The Receptors*. 1st ed. Cham: Springer International Publishing; Imprint: Humana.
- [55] Serrats J, Cunningham MO, Davies CH. GABAB receptor modulation to B or not to be B a pro-cognitive medicine? *Curr Opin Pharmacol*. 2017;35:125–32.
- [56] Legg B, Rowland M. Cyclosporin: measurement of fraction unbound in plasma. *J Pharm Pharmacol*. 1987;39:599–603.
- [57] Ptachcinski RJ, Venkataramanan R, Burckart GJ. Clinical pharmacokinetics of cyclosporin. *Clin Pharmacokinet*. 1986;11:107–32.
- [58] Wang CK, Stalmans S, De Spiegeleer B, Craik DJ. Biodistribution of the cyclotide MCoTI-II, a cyclic disulfide-rich peptide drug scaffold. *J Pept Sci*. 2016;22:305–10.